

Structural stability and improved properties of poly(3-alkylthiophenes) synthesized in an acid medium

Danielly Cristina Bento¹ · Guy Louarn² · Henrique de Santana¹

Received: 22 December 2015 / Accepted: 28 January 2016 / Published online: 2 February 2016
© Springer Science+Business Media New York 2016

Abstract Poly(3-methylthiophene) (P3MT), poly(3-hexylthiophene) (P3HT) and poly(3-octylthiophene) (P3OT), with better chemical stability, efficiency and charge transfer properties for use in organic solar cells were synthesized on indium tin oxide (ITO) in LiClO₄–acetonitrile (ACN) and in the presence of diphenyl phosphate (DHP), used as a Bronsted–Lowry acid. By means of cyclic voltammetry in the DHP–LiClO₄–ACN, we observed the displacement of two oxidation peaks, as well as the widening and definition of the second reduction peak in comparison to P3ATs synthesized in a neutral medium. Using electrochemical impedance spectroscopy, the Nyquist diagrams for the ITO/P3MT/DHP–LiClO₄–ACN system revealed a reduction in charge transfer resistance as the amount of DHP was increased. However, for ITO/P3HT/DHP–LiClO₄–ACN and ITO/P3OT/DHP–LiClO₄–ACN this dependence was not observed. In the Bode-phase diagrams, the charge transfer processes were related to polaronic conduction in the ITO/P3MT/DHP–LiClO₄–ACN, and bipolaronic conduction in the ITO/P3HT/DHP–LiClO₄–ACN and ITO/P3OT/DHP–LiClO₄–ACN. These results were complemented by ex situ Raman spectroscopy, in which the charge transfer process in the ITO/P3MT/DHP–LiClO₄–ACN system was due to radical cation species stabilization in the P3MT as prepared, and in the ITO/P3HT/DHP–LiClO₄–ACN and ITO/P3OT/DHP–LiClO₄–ACN systems it occurred

because of the stabilization of the dication on the P3HT and P3OT films obtained. The stability of these various species in the polymer matrix varied as time elapsed, leading to a disproportionate quantity of radical cation segments in aromatic and dication segments of the P3MT matrix, and the formation of a charge transfer complex with oxygen in the P3HT and P3OT. The radical cation segments stabilized 48 h after preparation.

1 Introduction

Poly(3-alkylthiophenes) (P3ATs) have been attracting a lot of interest in the field of organic optoelectronics due to their good charge transfer properties, chemical stability and photosensitivity to sunlight, making them good candidates for use in organic photovoltaics (OPVs) and other organic devices [1–6]. As π -conjugate systems, P3ATs are susceptible to structural variations, forming *p-type* doped conductor electron donor systems through oxidation [7–9]. This doping generates charge carriers such as radical cations (polaron) and dications (bipolaron) along the P3AT polymer chain, responsible for transporting the positive charge at the heterojunction in OPVs [10–26].

This has resulted not only in the need for studies on the efficiency of devices containing this material, but also the increased importance of the structural investigation of P3ATs and derived materials due to the different synthesis conditions used, contributing to an investigation of the stability of the material due to the atmospheric conditions it has to withstand, and helping to understand the electrochemical and charge transfer processes in these polymers, responsible for the efficiency of optoelectronic devices [2, 23, 27–30]. Working with P3ATs and copolymers of P3ATs and polydiphenylamine (PDFA), produced in

✉ Henrique de Santana
hensan@uel.br

¹ Departamento de Química, CCE, Universidade Estadual de Londrina, Londrina, PR 86051-990, Brazil

² Institut des Matériaux Jean Rouxel, Université de Nantes-CNRS, 44322 Nantes, France

different electrolytes and on different substrates (for instance, ITO and Pt), EIS was used to observe variations in charge transfer resistance. Raman spectroscopy was then used to compare displacements in the equilibrium of aromatic, radical cation and dication species in the polymer matrix of these new materials [23, 27, 30].

Since the electrical properties of P3ATs is determined by the segments present in the polymer matrix, the aim of this paper was to study the influence of diphenyl phosphate (DPHP) on the structural stabilization of these polymers. DPHP is referred to as a Bronsted-Lowry acid that facilitates proton exchange during electrochemical oxidation [31, 32]. De Santana et al. [33] investigated the behavior of *N,N'*-diphenyl-1,4-phenylenediamine in a DPHP acid medium using cyclic voltammetry, in situ UV-Vis spectroscopy and Raman spectroscopy. The authors detected a second cathodic peak on the cyclic voltammogram obtained in an acid medium, behavior that was not observed in CVs obtained in a neutral medium, and using Raman spectroscopy, they confirmed the existence of a differentiated mechanism in which aromatic and dication segments were stabilized in this material in the presence of DPHP.

In our study, polymer films of P3MT, P3HT and P3OT were synthesized on ITO in a $\text{LiClO}_4\text{-ACN}$ electrolyte, adding different concentrations of DPHP as the acid, with the aim of obtaining materials with stable polymer structures associated with improved electrical and optical properties for use in organic devices. The electrochemical behavior of three systems (ITO/P3MT/DPHP- $\text{LiClO}_4\text{-ACN}$, ITO/P3HT/DPHP- $\text{LiClO}_4\text{-ACN}$ and ITO/P3OT/DPHP- $\text{LiClO}_4\text{-ACN}$) was studied using cyclic voltammetry (CV), and charge transfer resistance processes monitored using electrochemical impedance spectroscopy (EIS). From the EIS results obtained, the charge transfer resistance values (R_{CT}) of the systems at open circuit potential were determined on the Nyquist diagrams. Then the data obtained from EIS were used for studying time constants by means of Bode phase diagrams to help identify the charge transfer processes in which polaron conduction (radical cation) and bipolaron conduction (dication) could be associated at low frequencies, representing the displacement of positive charges in the polymer matrix [34–36]. In conjunction with EIS, ex situ Raman spectroscopy was used to elucidate the influence of the DPHP acid medium on the stabilization of aromatic, radical cation and dication in the polymer matrix by comparison with films generated in a neutral medium, and on the redox and charge transfer processes observed in the CVs, Nyquist and Bode-phase diagrams of the systems obtained in DPHP. Raman spectroscopy was also used to monitor the time-dependent stability of the various species present

in the P3AT polymer matrices synthesized in DPHP, since due to the chemical nature of the polymer and the environmental conditions under which it was stored, the structure can undergo alterations induced by natural dedoping as time progresses [2, 28, 29].

2 Experimental design

2.1 Reagents

Monomers 3-methylthiophene ($\text{C}_5\text{H}_7\text{S}$), 3-hexylthiophene ($\text{C}_{10}\text{H}_{16}\text{S}$) and 3-octylthiophene ($\text{C}_{12}\text{H}_{20}\text{S}$) were used as received from the supplier, Aldrich. The support electrolyte was used in neutral and acid medium. The neutral medium, $\text{LiClO}_4\text{-ACN}$, consisted of 99 % lithium perchlorate (LiClO_4) supplied by Acros Organics in 99.5 % HPLC grade acetonitrile (ACN) solvent obtained from JT Baker. The acid medium, DPHP- $\text{LiClO}_4\text{-ACN}$, consisted of 99 % diphenyl phosphate [$(\text{C}_6\text{H}_5\text{O})_2\text{P}(\text{O})\text{OH}$] from Aldrich, used at concentrations ranging from 0.020 to 0.100 mol L^{-1} in $\text{LiClO}_4\text{-ACN}$.

2.2 Synthesis by chronoamperometry (CA) and investigation by cyclic voltammetry (CV)

The monomer solutions (3-methylthiophene, 3-hexylthiophene and 3-octylthiophene) were prepared in a $\text{LiClO}_4\text{-ACN}$ neutral medium and a DPHP- $\text{LiClO}_4\text{-ACN}$ acid medium. The P3MT, P3HT and P3OT films were electrochemically synthesized on ITO, with an average surface area of 0.30 cm^2 . All potentials were determined by reference to the Ag/AgCl in a Luggin Capillary in a 0.100 mol L^{-1} solution of LiClO_4 in acetonitrile ($\text{LiClO}_4\text{-ACN}$). For the purpose of CV, the electrolytic solution was used in a $\text{LiClO}_4\text{-ACN}$ neutral medium and in a DPHP- $\text{LiClO}_4\text{-ACN}$ acid medium.

The conditions under which the P3MT, P3HT, P3OT films were electrochemically synthesized are given in Table 1.

The CA and CV curves were obtained using an Autolab PGSTAT 302 N potentiostat/galvanostat connected to a microcomputer running NOVA 1.8.

2.3 Electrochemical impedance spectroscopy (EIS)

The open circuit potential (OCP) impedance diagrams were obtained on an Autolab PGSTAT 302 N potentiostat with a FRAM32 impedance module, varying the frequency from 100 kHz to 0.01 Hz.

The maximum frequency values (f) and OCP for each system during EIS are given in Table 2.

Table 1 Experimental conditions for chronoamperometry (CA) synthesis of films on ITO

Films	Concentration (mol L ⁻¹)			Time (s)	E (V vs. Ag/AgCl)	J (mA cm ⁻²)
	3MT	3HT	3OT			
P3MT	0.035	–	–	180	1.65	2.60
P3HT	–	0.040	–	180	1.75	2.06
P3OT	–	–	0.040	180	1.80	2.45

Table 2 Maximum frequency (*f*) and open circuit potential (OCP) values for the polymers

Films	<i>f</i> (Hz)				OCP _(vs. a)			
	DHPH (mol L ⁻¹)				DHPH (mol L ⁻¹)			
	0.020	0.040	0.060	0.100	0.020	0.040	0.060	0.100
P3MT	7943	12,589	15,849	12,589	0.69	0.76	0.69	0.68
P3HT	1.99	316	6.31	2.51	0.63	0.61	0.53	0.54
P3OT	25.12	0.79	0.10	2.51	0.63	0.60	0.57	0.61

2.4 Spectroscopic characterization

The Raman spectra were obtained on an Advantage532[®] portable Raman spectrometer (DeltaNu), excited at 532 nm with resolution of 8 cm⁻¹. NuSpec software (DeltaNu) and baseline resources used to remove background fluorescence.

3 Results

Figure 1 shows the cyclic voltammograms obtained for the P3MT, P3HT and P3OT films on ITO at 0.100 mol L⁻¹ of LiClO₄-ACN acidified with 0.100 mol L⁻¹ diphenyl phosphate (DHPH). For comparison, these voltammograms are shown with the data for the P3MT, P3HT and P3OT films synthesized in 0.100 mol L⁻¹ of LiClO₄-ACN obtained in the earlier study [27]. The voltammograms are relative to the first scan and begin at -1.50 V.

Comparing the cyclic voltammogram for P3MT synthesized on ITO in DHPH-LiClO₄-ACN with the ITO/P3MT/LiClO₄-ACN system in Fig. 1a, there are two clearly-defined oxidation peaks at +0.80 and +2.00 V, with the first peak displaced relative to the peak observed without the DHPH, from +1.50 to +0.80 V. Reduction of the ITO/P3MT/DHPH-LiClO₄-ACN shows a single peak centered at +0.24 V, which is merely wider than the reduction peak for P3MT synthesized in LiClO₄-ACN.

In previous studies, the oxidation peak at +1.50 V for the ITO/P3MT/LiClO₄-ACN system was related to the stabilization of the radical cation in the polymer film [27]. The shift in this peak to a potential of +0.80 V could indicate that the presence of the DHPH, acting as a Bronsted-Lowry acid, is helping stabilize these species in the

polymer matrix, as observed for *N,N'*-diphenyl-1,4-phenylenediamine and polydiphenylamine [33, 37].

In Fig. 1b, the cyclic voltammogram of P3HT synthesized in DHPH-LiClO₄-ACN compared to the P3HT produced in LiClO₄-ACN shows two oxidation peaks at +1.05 and +1.80 V, that are displaced from the potentials of +1.17 and +1.90 V seen in the polymer synthesized in LiClO₄-ACN. During reduction, we also observed two peaks at +0.06 and +0.70 V, but the polymer synthesized in LiClO₄-ACN exhibits only one peak at -0.09 V.

For the ITO/P3OT/DHPH-LiClO₄-ACN system, Fig. 1c shows two oxidation peaks displaced to +1.14 and +1.66 V, compared to the peaks at +1.00 and +2.00 V for the P3OT synthesized in LiClO₄-ACN. Furthermore, in the acid medium there are two reduction peaks at +0.14 and +0.69 V, but in the neutral medium there is only one peak at +0.78 V.

Similar to the observations made for the ITO/P3HT/LiClO₄-ACN and ITO/P3OT/LiClO₄-ACN systems, the second oxidation peaks at +1.80 e +1.66 V for the ITO/P3HT/DHPH-LiClO₄-ACN and ITO/P3OT/DHPH-LiClO₄-ACN systems are related to the stabilization of the dication in the polymer film [27]. The shifts in the second peaks for the P3HT and P3OT synthesized in the acid medium could show that the presence of DHPH is helping stabilize the dication in the polymer matrix.

Therefore, the reduction of the dication species to radical cation, and subsequently of the radical cation to neutral was helped in the acid medium (DHPH-LiClO₄-ACN) due to stabilization of the dication. Conversely, in the neutral solution (LiClO₄-ACN) there may have been chemical reactions or degradation to the dication or radical cation segments, preventing dication reduction on the surface of the electrode, resulting in only one reduction peak on the CVs [33].

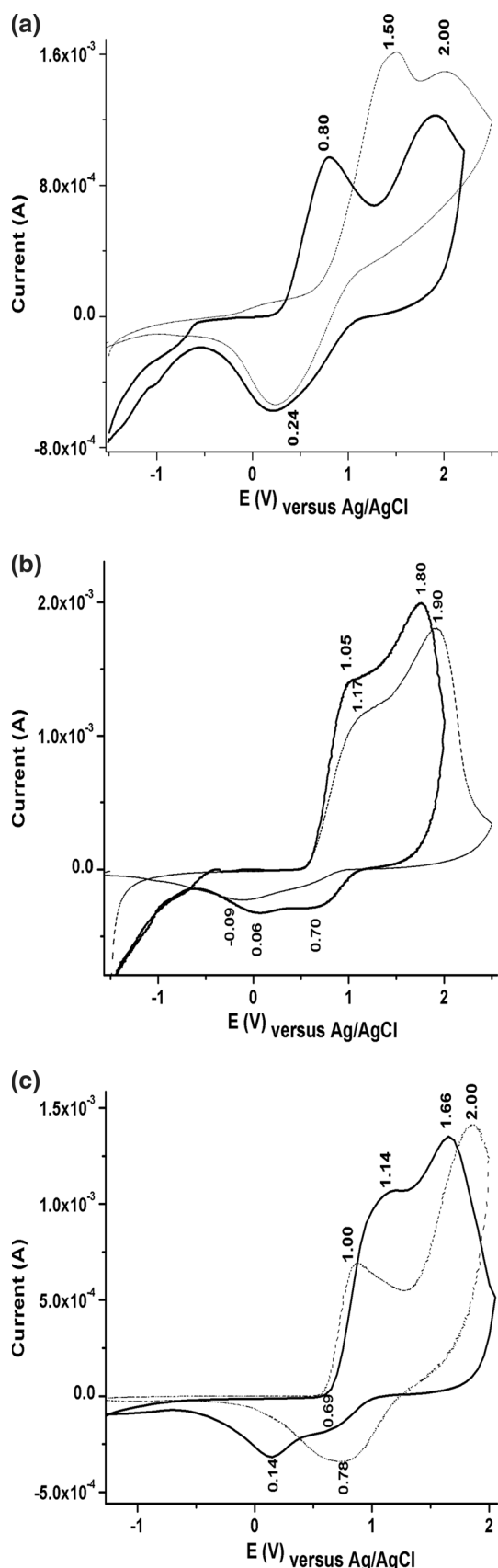


Fig. 1 Cyclic voltammograms of films of **a** P3MT, **b** P3HT and **c** P3OT synthesized on ITO in $0.100 \text{ mol L}^{-1} \text{ LiClO}_4 + 0.100 \text{ mol L}^{-1} \text{ DPHP}$ in acetonitrile (solid line); and $0.100 \text{ mol L}^{-1} \text{ LiClO}_4$ in acetonitrile (dashed line) (Bento et al. [10, 27]). $v = 50 \text{ mV s}^{-1}$

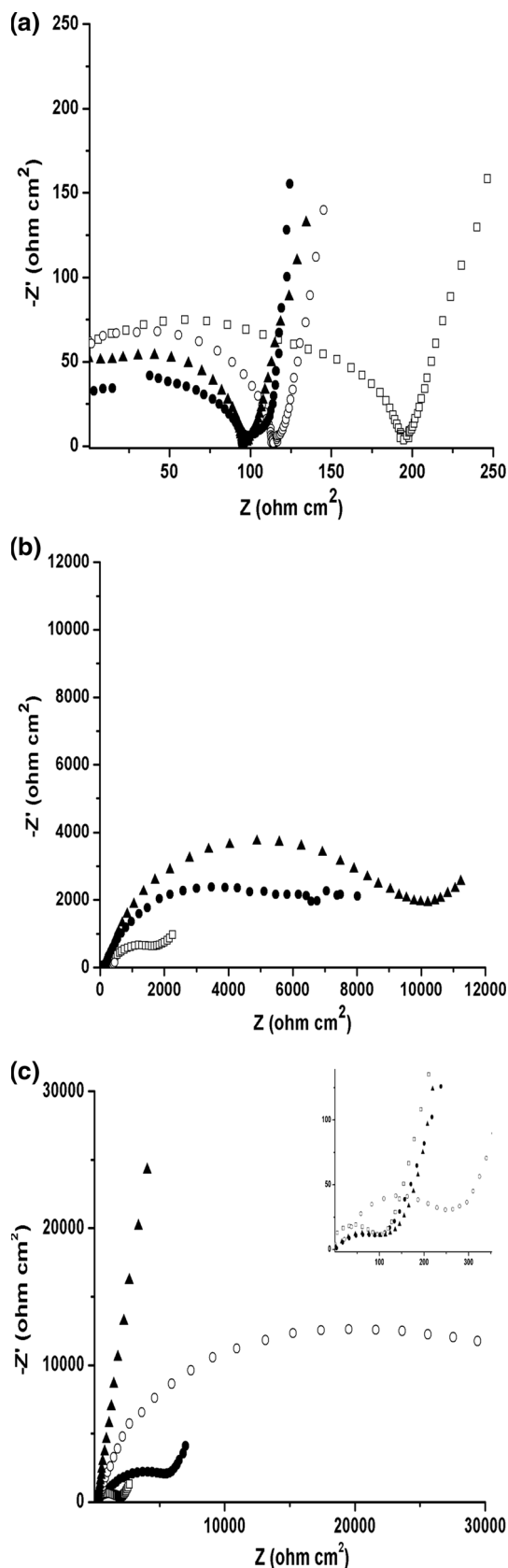
Figure 2 shows the Nyquist diagrams obtained after synthesizing the P3MT, P3HT and P3OT in 0.100 mol L^{-1} of $\text{LiClO}_4\text{-ACN}$ with the addition of $0.020\text{--}0.100 \text{ mol L}^{-1}$ of DPHP. The diagrams were obtained at open circuit potential (OCP).

The Nyquist diagrams in Fig. 2a, c (insert) for P3MT and P3OT show the formation of semicircles at high frequencies relating to the process of resistance to charge transfer at the ITO/P3ATs/DPHP- LiClO_4 interface. For P3HT and P3OT, Fig. 2b, c show the formation of semicircles at low frequencies relating to the process of resistance to charge transfer at the P3ATs/DPHP- LiClO_4 interface [34, 36]. The Nyquist diagram for P3HT in Fig. 2b shows the formation of only one semicircle at low frequencies. This could have occurred due to overlapping of the semicircles when the exchange reaction time constants are very close [36]. The same behavior was also observed in studies in which EIS was used to investigate P3ATs and their copolymers [23, 27, 34, 38].

In Fig. 2a, the Nyquist diagrams for the ITO/P3MT/DPHP- $\text{LiClO}_4\text{-ACN}$ system show the reduction in the semicircle diameter as the concentration of DPHP is increased in the solution. The R_{CT} values for this system with the addition of $0.020, 0.040, 0.060$ and 0.100 mol L^{-1} DPHP were $195.60, 111.06, 98.01$ and $94.40 \Omega \text{ cm}^2$ respectively. These values show how this system's R_{CT} is dependent on DPHP concentration. As from the addition of 0.040 mol L^{-1} DPHP, lower values of R_{CT} are observed in the ITO/P3MT/DPHP- $\text{LiClO}_4\text{-ACN}$ system by comparison with the ITO/P3MT/ $\text{LiClO}_4\text{-ACN}$ system in a neutral medium, that exhibited an R_{CT} value of $1.60 \times 10^2 \Omega \text{ cm}^2$ in previous studies [27].

The Nyquist diagrams for P3HT and P3OT in Fig. 2b, c, in contrast to the observations made for P3MT, showed no correlation between the concentration of DPHP and the increase in semicircle diameter. The results indicate that at acid concentrations of 0.060 mol L^{-1} for P3HT and 0.040 mol L^{-1} for P3OT, the ITO/P3HT/DPHP- $\text{LiClO}_4\text{-ACN}$ and ITO/P3OT/DPHP- $\text{LiClO}_4\text{-ACN}$ systems exhibit R_{CT} values of 5.38 and $22.10 \Omega \text{ cm}^2$, higher than the values for the ITO/P3HT/ $\text{LiClO}_4\text{-ACN}$ and ITO/P3OT/ $\text{LiClO}_4\text{-ACN}$ systems in a neutral medium, whereas these systems exhibited R_{CT} values of 1.81×10^3 and $1.34 \times 10^3 \Omega \text{ cm}^2$ in previous studies [27].

In view of the results obtained for the systems containing P3MT, P3HT and P3OT in a DPHP medium, there



◀**Fig. 2** Nyquist diagrams obtained at OCP for films of **a** P3MT, **b** P3HT and **c** P3OT synthesized on ITO in 0.100 mol L⁻¹ LiClO₄+ (open square) 0.020, (open circle) 0.040, (filled triangle) 0.060 and (filled circle) 0.100 mol L⁻¹ DPHP in acetonitrile

was a significant increase in semicircle diameter in the Nyquist diagrams for the poly(3-alkylthiophenes) with a longer side chain, giving the systems with P3HT and P3OT a higher R_{CT} . In studies on the charge transfer behavior in poly(3-alkylthiophenes) using different alkyl substituents, Park et al. [39] observed that charge carrier mobility decreases as the alkyl side chain lengthens in these materials. Thus the increase in R_{CT} in systems containing P3HT and P3OT by comparison with the R_{CT} of the system containing P3MT is due to the alkyl substituent of these materials, which has a major effect on the electrical properties of P3AT-based devices [40, 41].

The Bode-phase diagrams based on the data produced by EIS at OCP are given in Fig. 3 for the P3AT films with the addition of different concentrations of DPHP. These diagrams were produced with the aim of elucidating the charge transfer processes in relation to polaronic and bipolaronic conduction.

The Bode-phase diagram for the ITO/P3MT/DPHP–LiClO₄–ACN in Fig. 3a shows the two phases relating to polaronic conduction at low frequency and electronic conduction at high frequency [27, 35]. This behavior was observed for all systems of ITO/P3MT/DPHP–LiClO₄–ACN subjected to EIS in LiClO₄–ACN at different concentrations of DPHP, and no phase alterations were observed as the concentration of DPHP was increased.

The Bode-phase diagram for the ITO/P3HT/DPHP–LiClO₄–ACN system in Fig. 3b shows the phases relating to bipolaronic and electronic conduction. In contrast to the Bode-phase diagram for ITO/P3MT/DPHP–LiClO₄–ACN, in the case of ITO/P3HT/DPHP–LiClO₄–ACN there is a phase related to bipolaronic conduction that shifts to lower frequencies as the concentration of DPHP varies. Thus the phase relating to bipolaronic conduction was observed with the addition of DPHP of 0.020 mol L⁻¹ at 469.00 Hz, 0.040 mol L⁻¹ at 8.22 and 240.00 Hz, 0.060 mol L⁻¹ at 55.62 Hz and 0.100 mol L⁻¹ at 19.45 Hz. This phase displacement at lower frequencies as the concentration of DPHP is increased could be due to the contribution made by polaronic conduction to the charge transfer processes in this system [34].

In Fig. 3c, the Bode-phase diagram for the ITO/P3OT/DPHP–LiClO₄–ACN system shows that as the DPHP is increased, this displaces the phase related to bipolaronic conduction at lower frequencies. When compared to the

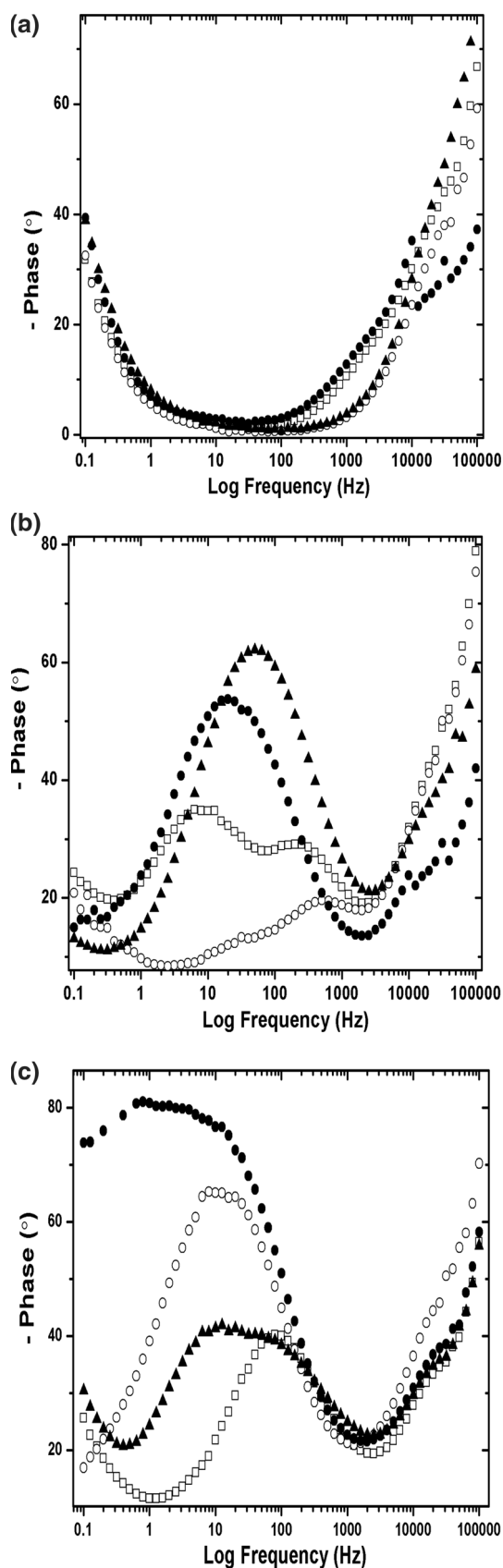


Fig. 3 Bode-phase diagrams for **a** P3MT, **b** P3HT and **c** P3OT synthesized on ITO in $0.100 \text{ mol L}^{-1} \text{ LiClO}_4$ + (open square) 0.020 , (open circle) 0.040 , (filled triangle) 0.060 and (filled circle) 0.100 mol L^{-1} DPHP in acetonitrile

diagram for the ITO/P3HT/DPHP– LiClO_4 –ACN system and at the same DPHP concentrations, there are phases at lower frequencies: at 0.020 mol L^{-1} there is a phase at 85.00 Hz , at 0.040 mol L^{-1} at 14.00 Hz , at 0.060 mol L^{-1} at 31.00 Hz and at 0.100 mol L^{-1} at 2.00 Hz . Thus as the DPHP concentration is increased in the ITO/P3OT/DPHP– LiClO_4 –ACN system, polaronic conduction makes a greater contribution to the charge transfer process in this system than in the ITO/P3HT/DPHP– LiClO_4 –ACN system.

The displacement observed in the phase relating to bipolaronic conduction towards polaronic conduction in the Bode-phase diagrams for the ITO/P3HT/DPHP– LiClO_4 –ACN and ITO/P3OT/DPHP– LiClO_4 –ACN systems indicates that the process occurred in two stages, as revealed in the previous study complemented by in situ Raman spectroscopy [2, 3]. Therefore, these stages are associated with oscillations in radical cation and dication species in the P3HT and P3OT matrices as the DPHP concentration is increased.

To complement studies of the electrochemical behavior of P3MT, P3HT and P3OT in the presence of different concentrations of DPHP, ex situ Raman spectroscopy is discussed below with a view to elucidating the influence of these quinone and semiquinone species in these materials.

Figure 4 shows the Raman spectra for the films synthesized in DPHP– LiClO_4 –ACN at DPHP concentrations ranging from 0.020 to 0.100 mol L^{-1} . The 1400 – 1500 cm^{-1} region was investigated since it is ascribed to the C=C symmetric stretching of the thiophene ring and this mode is sensitive to changes in the thiophene ring when aromatic, radical cation and dication species vary in the polymer matrix of P3ATs [2, 27, 42, 43].

The spectra obtained shortly after electrochemical synthesis of the P3MT (Fig. 4a) with the addition of 0.020 and 0.040 mol L^{-1} DPHP show a band centered on 1479 cm^{-1} attributed to the radical cation species present in the P3MT polymer matrix [27]. Increasing the concentration of DPHP resulted in the displacement of this band to 1483 cm^{-1} , showing the dependence of radical cation stabilization on the concentration of DPHP. This behavior conflicts with the observations made in the previous study, in which the P3MT synthesized on ITO in LiClO_4 –ACN exhibited bands at 1438 and 1461 cm^{-1} relating respectively to the aromatic and dication segments [27].

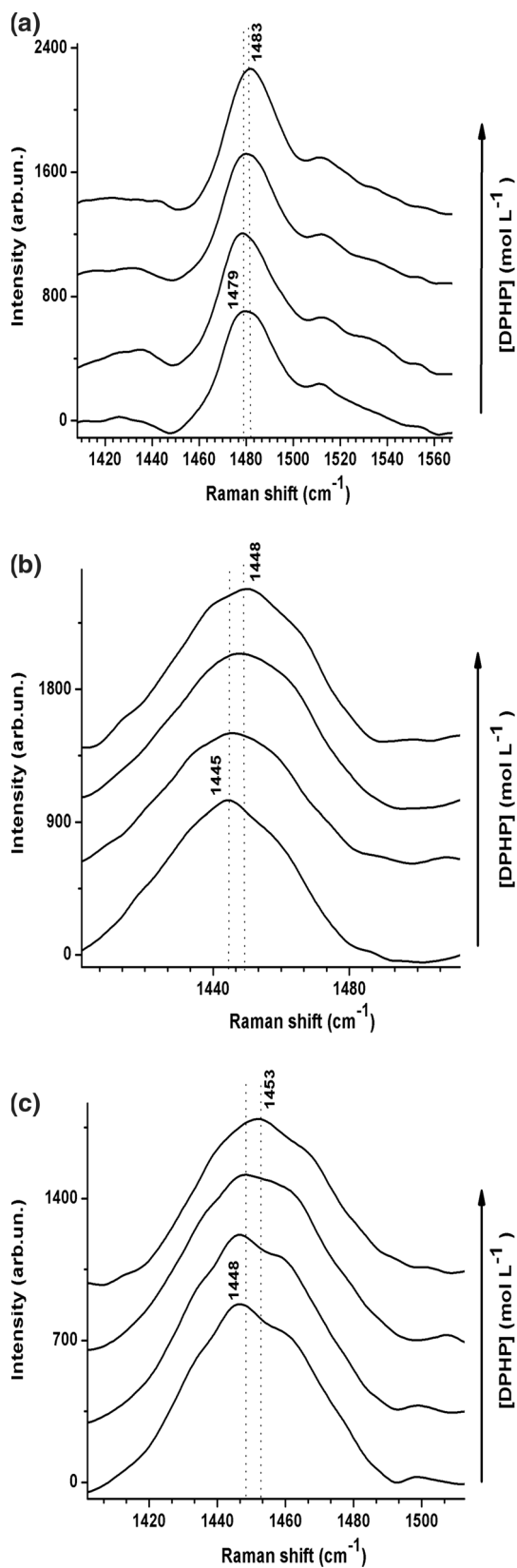


Fig. 4 Raman spectra obtained soon after synthesis of films of **a** P3MT, **b** P3HT and **c** P3OT on ITO in 0.100 mol L⁻¹ LiClO₄ + DHPH 0.020–0.100 mol L⁻¹ in ACN

Therefore, these results show that the reduction in R_{CT} in the Nyquist diagrams (Fig. 2a) and the occurrence of only polaronic phases in the Bode-phase diagram (Fig. 3a) may be related to the stabilization of the radical cation in the P3MT film when synthesized in a DPHP acid medium. This lower R_{CT} value could be due to increased diffusion-migration of the ClO₄⁻ dopant due to the higher interaction between positively charged segments and this countering [23], helping increase charge transfer in the ITO/P3MT/DPHP–LiClO₄–ACN system.

The Raman spectra obtained for the P3HT and P3OT films (Fig. 4b, c) synthesized at a low concentrations of DPHP showed bands at 1445 and 1448 cm⁻¹ attributed respectively to the dication species in the P3HT and P3OT [27]. As the concentration of DPHP was increased in the synthesis of the P3HT and P3OT films, these bands are displaced respectively to 1448 and 1453 cm⁻¹.

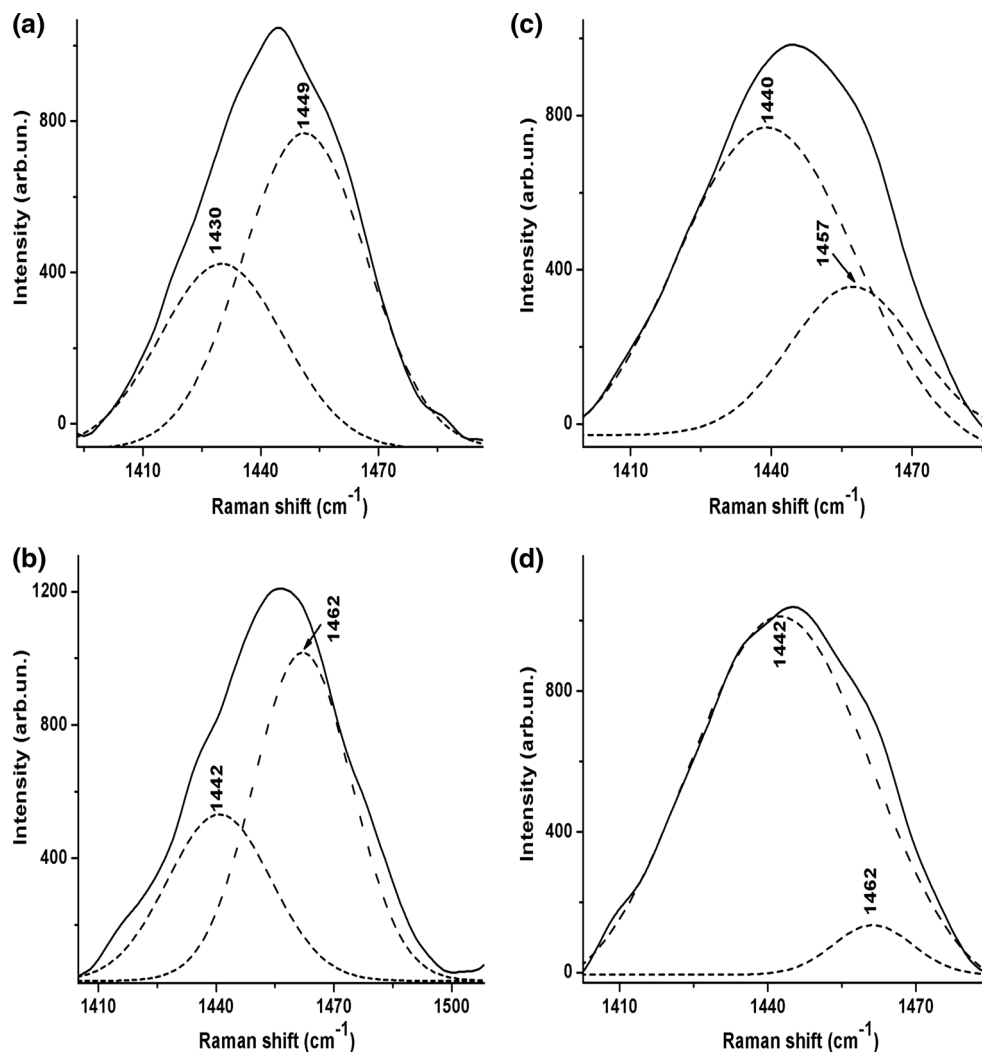
In view of the displacement and widening observed in the Raman spectra of P3HT and P3OT as the DPHP concentration is varied, it was necessary to deconvolute the spectral region studied, in order to better elucidate the structural alterations that could have taken place in the P3HT and P3OT polymer matrices when synthesized at different concentrations of DPHP.

Figure 5 shows the deconvolutions of the Raman spectra of P3HT synthesized in DPHP–LiClO₄–ACN at DPHP concentrations ranging from 0.020 to 0.100 mol L⁻¹.

The deconvoluted Raman spectra of the P3HT synthesized at different DPHP concentrations (Fig. 5) show bands centered on 1422–1430, 1440–1449 and 1454–1462 cm⁻¹ ascribed respectively to the aromatic, dication and radical cation species, as in previous Raman spectroscopy studies of the P3HT film on ITO [27]. The intensity of these bands varies, with the highest intensity in the band attributed to the dication in the spectra of the P3HT films synthesized at higher concentrations of DPHP (Fig. 5c, d). These results show that under these conditions, the dication segment stabilizes in the P3HT polymer matrix. This confirms that the definition of the second cathodic peak observed in the CV of the P3HT film produced by adding 0.100 mol L⁻¹ DPHP (Fig. 1b) is due to the electrochemical reduction on the electrode surface of stabilized dication segments in this medium.

Figure 5a shows bands centered at 1430 and 1449 cm⁻¹ respectively related to the stabilization of aromatic and dication species in the spectrum of the P3HT film synthesized by adding 0.020 mol L⁻¹ DPHP. Thus we can confirm that the charge transfer process in this system is controlled by stabilization of the dication responsible for bipolaronic conduction, as seen in the Bode-phase diagram of the ITO/P3HT/DPHP–LiClO₄–ACN system with 0.020 mol L⁻¹ DPHP (Fig. 3b).

Fig. 5 Deconvoluted Raman spectra of films obtained after synthesis of P3HT on ITO in $0.100 \text{ mol L}^{-1} \text{ LiClO}_4 +$ **a** 0.020 ; **b** 0.040 ; **c** 0.060 and **d** 0.100 mol L^{-1} DPHP in ACN



As the concentration of DPHP is increased when synthesizing P3HT, the deconvoluted Raman spectra showed a radical cation band at $1457\text{--}1462 \text{ cm}^{-1}$. In the Raman spectrum of the film synthesized at 0.040 mol L^{-1} DPHP (Fig. 5b), the band related to the radical cation is more intense than that of the dication, characterizing this system as having a lower charge transfer resistance than the other systems synthesized with DPHP. This explains the data in the Bode-phase diagram of the ITO/P3HT/DPHP– LiClO_4 –ACN system (Fig. 3b), in which the presence of the dication species is responsible for the phase at 240.00 Hz related to bipolaronic conduction, and the stabilized radical cation species in the P3HT polymer film is therefore responsible for the phase at 8.22 Hz related to polaronic conduction when synthesized at 0.040 mol L^{-1} DPHP.

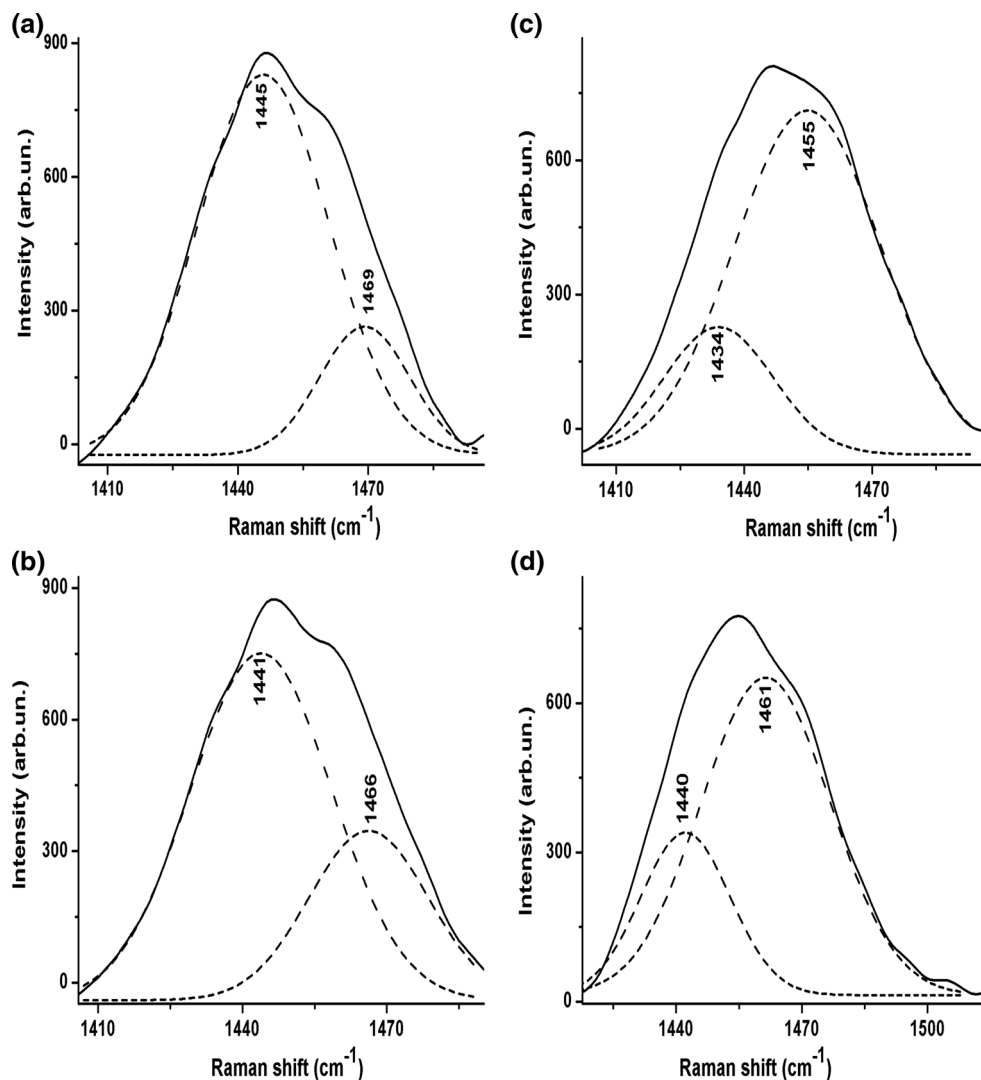
However, at concentrations of 0.060 and 0.100 mol L^{-1} DPHP (Fig. 5c, d), the intensity of the dication band was higher than that of the radical cation. Therefore, at these DPHP concentrations, the dication species is more stable in

the P3HT polymer film. In line with previous studies [23, 27], we can confirm that a higher quantity of the dication species in the P3HT polymer matrix helps increase R_{CT} in the ITO/P3HT/DPHP– LiClO_4 –ACN system (Fig. 2b). Using the deconvoluted Raman spectra data, it was also possible to relate the bipolaronic conduction phase observed in the Bode-phase diagram (Fig. 3b) and its displacement to the polaronic conduction phase in this system to the presence of the dication and radical cation in the P3HT when synthesized at these DPHP concentrations.

For the P3OT films synthesized at different DPHP concentrations, we also obtained Raman spectra shortly after synthesis. Figure 6 shows the deconvoluted spectra of P3OT synthesized in DPHP– LiClO_4 –ACN at DPHP concentrations ranging from 0.020 to 0.100 mol L^{-1} .

Figure 6a–d show the deconvoluted Raman spectra obtained shortly after synthesis of the P3OT film at different DPHP concentrations, with bands at $1428\text{--}1438$, $1440\text{--}1445$ and $1455\text{--}1469 \text{ cm}^{-1}$ attributed respectively to

Fig. 6 Deconvoluted Raman spectra of films obtained after synthesis of P3OT on ITO in $0.100 \text{ mol L}^{-1} \text{ LiClO}_4 +$ **a** 0.020 ; **b** 0.040 ; **c** 0.060 and **d** 0.100 mol L^{-1} DPHP in ACN



the aromatic, dication and radical cation species present in the P3OT polymer matrix [27]. As observed for P3HT, the Raman spectra of P3OT synthesized at 0.100 mol L^{-1} DPHP showed a band at 1440 cm^{-1} ascribed to the presence of the dication. The presence of this species in the P3OT results in a second reduction peak, as shown in the CV of the film produced at 0.100 mol L^{-1} DPHP (Fig. 1c).

Deconvoluting the Raman spectrum obtained shortly after synthesizing the sample of P3OT synthesized at 0.020 mol L^{-1} DPHP (Fig. 6a) showed the dication and radical cation bands at 1455 and 1469 cm^{-1} respectively, at different relative intensities. The band relating to the dication at 1455 cm^{-1} was more intense. These synthesis conditions therefore helped stabilize the dication species in the polymer film. This stabilization proves that the charge transfer process in the ITO/P3OT/DPHP– LiClO_4 –ACN

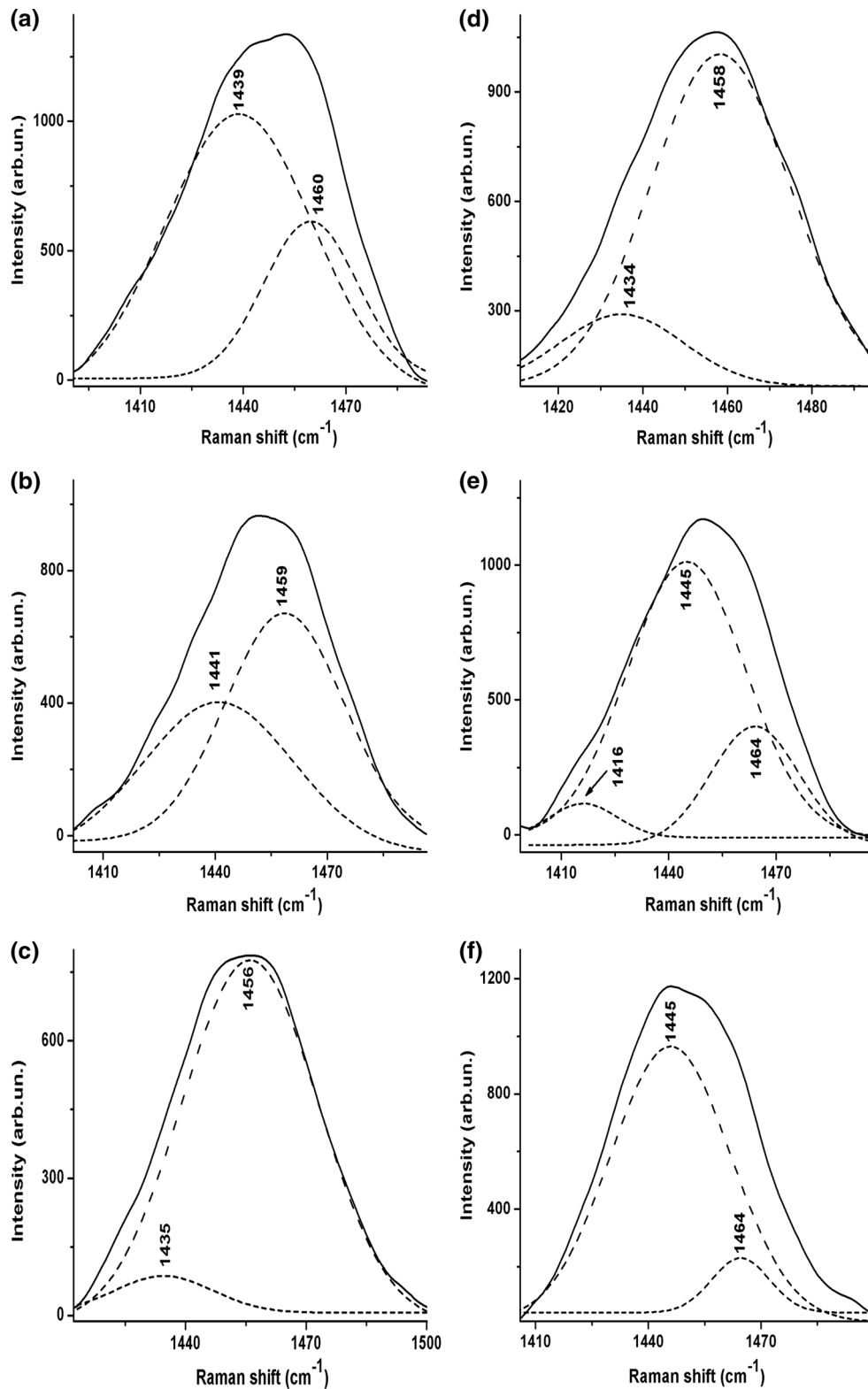
system at 0.020 mol L^{-1} DPHP is due to the bipolaronic conduction process (Fig. 3d) controlled by the dication species.

As the concentration of DPHP is increased in the synthesis of P3OT, the deconvoluted Raman spectra (Fig. 6c, d) show that the intensity of the band relating to the radical cation is higher than that of the dication, indicating that higher concentrations of DPHP produce greater stabilization of the radical cation segment in the P3OT matrix, and that this is responsible for the displacement of the phase relating to bipolaronic conduction (dication) at lower frequencies in which polaronic conduction is responsible for charge transfer in the ITO/P3OT/DPHP– LiClO_4 –ACN system (Fig. 6d). This explains why the phase constant displacements in the Bode-phase diagram at lower frequencies in the ITO/P3OT/DPHP– LiClO_4 –ACN system is greater than in the ITO/P3HT/DPHP– LiClO_4 –ACN system,

due to the stability of the radical cation which, at higher DPHP concentrations, shows greater stabilization than the dication species (Fig. 5c, d).

In addition to studying the influence of different concentrations of DPHP on the synthesis of P3ATs, we also observed the stability of various species in the polymer

Fig. 7 Deconvoluted Raman spectra of films 48 h after synthesis on ITO **a** P3MT, **b** P3HT and **c** P3OT synthesized in an acid medium of $\text{LiClO}_4 + 0.100 \text{ mol L}^{-1}$ DPHP in ACN; **d** P3MT, **e** P3HT and **f** P3OT synthesized in a neutral medium of $0.100 \text{ mol L}^{-1} \text{ LiClO}_4\text{-ACN}$



matrix at given times after synthesis in DPHP, based on the findings of Koizumi et al. [29] that P3ATs could undergo natural dedoping as time progresses, caused by the instability of the material due to its polymer nature, the length of the alkyl chain, humidity and the ambient conditions to which the films were subjected [2, 28, 29].

Figure 7 shows the deconvoluted Raman spectra of the P3MT, P3HT and P3OT films synthesized in neutral and DPHP medium and recorded 48 h after preparation. As mentioned above for the Raman spectrum of the P3MT film as prepared (Fig. 4a), the band at 1483 cm^{-1} associated with the radical cation was fairly predominant. However, after 48 h, this band was found to have widened and become displaced to a value centered on 1452 cm^{-1} . Figure 7a shows the deconvoluted Raman spectrum with bands at 1439 and 1460 cm^{-1} , as also observed in the spectrum of the P3MT synthesized in a neutral medium (Fig. 4d), in which the bands at 1434 and 1458 cm^{-1} are attributed to the aromatic and radical cation species. This time-dependent behavior of the film synthesized in an acid medium was probably a response to the disproportionality of the radical cation species in aromatic and dication segments, as observed in the literature on polydiphenylamine and phenyl capped dimer (of polyaniline) indicating that the proton also plays a key role in the process [33, 37].

As previously observed in deconvoluted Raman spectra obtained soon after the synthesis of the P3HT and P3OT films in DPHP–LiClO₄–ACN (Figs. 5, 6d), bands were found respectively at 1442 and 1462 cm^{-1} and at 1440 and 1461 cm^{-1} , with different relative intensities. Therefore, soon after synthesis, it was found that the P3HT spectrum showed higher intensity of the dication band at 1442 cm^{-1} and the P3OT spectrum a set of bands attributed to the dication and radical cation, the latter being the most intense.

However, the deconvoluted Raman spectra of the P3HT and P3OT films stored for 48 h under atmospheric conditions (Fig. 7b, c) showed a respective predominance of frequencies at 1459 and 1456 cm^{-1} , indicating that the radical cation species stabilizes in the polymer matrix naturally as time progresses. This behavior was not observed in films of P3HT and P3OT synthesized in a neutral medium, in which the most intense band attributed to the dication was at 1445 cm^{-1} (Fig. 7e, f). Abdou et al. [44] suggested that there is diffusion of molecular oxygen through the P3HT matrix, favorable to the formation of a charge transfer complex (CTC) between the electrons delocalized on the polymer backbones and oxygen radical anions. The results obtained led us to the conclusion that the stability of the radical cation segments in the sample of P3OT and P3HT synthesized in the acid medium was

responsible for the formation of this CTC as time progresses.

4 Conclusion

The results of cyclic voltammetry, electrochemical impedance spectroscopy and Raman spectroscopy indicate that synthesizing poly(3-alkylthiophenes) in a DPHP acid medium results in polymer material with electrochemical and structural properties that differ from those observed in P3ATs synthesized in a neutral medium.

The cyclic voltammograms of the P3MT, P3HT and P3OT polymers synthesized in a DPHP acid medium show the displacement of two oxidation peaks as well as widening and clearer definition of the second reduction peak, compared to the CVs of P3ATs synthesized in a neutral medium. Raman spectroscopy revealed that these variations occur in the acid medium because of the stabilization of the radical cation species in the P3MT and stabilization of the dication in the P3HT and P3OT.

In the ITO/P3MT/DPHP–LiClO₄–ACN system subjected to increments in DPHP concentration, the Nyquist diagrams revealed a reduction in R_{CT} . In the ITO/P3HT/DPHP–LiClO₄–ACN and ITO/P3OT/DPHP–LiClO₄–ACN systems, dependence of R_{CT} on the DPHP concentration was not observed. In the Bode-phase diagrams, the charge transfer properties in the DPHP medium occurred due to polaronic conduction in the ITO/P3MT/DPHP–LiClO₄–ACN, and bipolaronic conduction in the ITO/P3HT/DPHP–LiClO₄–ACN and ITO/P3OT/DPHP–LiClO₄–ACN. The ex situ Raman spectroscopy data lead to the conclusion that the charge transfer process in the ITO/P3MT/DPHP–LiClO₄–ACN system is due to stabilization of the radical cation species in the P3MT film as prepared, and in the ITO/P3HT/DPHP–LiClO₄–ACN and ITO/P3OT/DPHP–LiClO₄–ACN systems, it was due to stabilization of the dication species in the P3HT and P3OT films obtained.

The Raman spectra also show that the radical cation segments in the P3MT matrix are disproportionate in the aromatic and dication segments, and for the P3HT and P3OT films, revealed that formation of the charge transfer complex with oxygen led to stabilization of radical cation segments 48 h after synthesis. Therefore, the stability of the radical cation segments in the P3HT and P3OT, boosting charge transfer, means that this film can be recommended for the active layer in OPVs.

Acknowledgments We would like to express our appreciation to the Spectroscopy Laboratory (SPEC) at the PROPPG/UEL Multiuser Center and the National Council for Scientific and Technological Development (CNPq) for their financial support (Project No.

441689/2014-0). D. C. Bento is indebted to the Coordination for the Improvement of Higher Education Personnel (CAPES) for the grant.

References

1. E. Zhou, Z. Tan, Y. He, C. Yang, Y. Li, *J. Polym. Sci. Part A Polym. Chem.* **45**, 629 (2007)
2. H. De Santana, E.C.R. Maia, D.C. Bento, T.N.M. Cervantes, G.J. Moore, *J. Mater. Sci. Mater. Electron.* **24**, 3352 (2013)
3. D.C. Bento, E.C.R. Maia, T.N.M. Cervantes, R.V. Fernandes, E. Di Mauro, E. Laureto, M.A.T. Da Silva, J.L. Duarte, I.F.L. Dias, H. de Santana, *Synth. Methods* **162**, 2433 (2012)
4. C.H. Kim, K. Kisie, J. Jung, J. Ulansk, D. Tondeliera, B. Gefroya, Y. Bonnassieuxa, G. Horowitza, *Synth. Methods* **162**, 460 (2012)
5. P. Vanlaeke, A. Swinnen, I. Haeldermans, G. Vanhoyland, T. Aernouts, D. Cheyins, C. Deibel, J. D'Haen, P. Heremans, J.S. Poortman, J.V. Manca, *J. Sol. Energy Mater. Sol. Cells* **90**, 2150 (2006)
6. F.M. Nodari, R.L. Patyk, L.S. Roman, A.R.V. Benvenho, I.A. Hummelgen, E.K.C. Yoshikawa, J. Gruber, *J. Mater. Sci. Mater. Electron.* **21**, 1235 (2010)
7. J.D. Stenger-Smith, *Prog. Polym. Sci.* **23**, 57 (1998)
8. L.H.C. Mattoso, *Quim. Nova* **19**, 388 (1996)
9. A. Ray, A.F. Richter, A.G. MacDiarmid, A.J. Epstein, *Synth. Methods* **29**, E151 (1989)
10. D.C. Bento, E.A. Da Silva, C.A. Olivati, G. Louarn, H. De Santana, *J. Mater. Sci. Mater. Electron.* **26**, 7844 (2015)
11. O.J. Alley, M.-Y. Wu, G.L. Johns, T.J. Dawidczyk, J.F.M. Hardigree, N. Markovic, M.S. Arnold, H.E. Katz, *Appl. Phys. Lett.* **106**, 033301 (2015)
12. L.-M. Chen, Z. Hong, G. Li, Y. Yang, *Adv. Mater.* **21**, 1434 (2009)
13. M.-C. Chen, S. Kar, D.-J. Liaw, W.-H. Chen, Y.-C. Huang, Y. Tai, *Org. Electron.* **13**, 2702 (2012)
14. C.L. Chochos, S.A. Choulis, *Prog. Polym. Sci.* **36**, 1326 (2011)
15. P. Morvillo, I.A. Grimaldi, R. Diana, F. Loffredo, F. Villani, *J. Mater. Sci.* **48**, 2920 (2013)
16. P. Veerender, V. Saxena, A.K. Chauhan, S.P. Koiry, P. Jha, A. Gusain, S. Choudhury, D.K. Aswal, S.K. Gupta, *J. Sol. Energy Mater. Sol. Cells* **120**, 526 (2014)
17. J. Yang, D. Vak, N. Clark, J. Subbiah, W.W.H. Wong, D.J. Jones, S.E. Watkins, G. Wilson, *Sol. Energy Mater. Sol. Cells* **109**, 47 (2013)
18. K. Marumoto, N. Takeuchi, T. Ozak, S. Kuroda, *Synth. Methods* **129**, 239 (2002)
19. A.A. Zakhidov, T. Akashia, K. Yoshino, *Synth. Methods* **70**, 1519 (1995)
20. H. Kuzmany, R. Pfeiffer, M. Hulman, C. Kramberger, *Phil. Trans. R. Soc. Lond. A* **362**, 2375 (2004)
21. S. Falke, P. Eravuchira, A. Materny, C. Lienau, J. Raman Spectrosc. **42**, 1897 (2011)
22. S. Bertho, B. Campo, F. Piersimoni et al., *Sol. Energy Mater. Sol. Cells* **110**, 69 (2013)
23. T.N.M. Cervantes, D.C. Bento, E.C.R. Maia, R.V. Fernandes, E. Laureto, G.J. Moore, G. Louarn, H. De Santana, *J. Mater. Sci. Mater. Electron.* **25**, 1703 (2014)
24. A. Tarola, D. Dini, E. Salatelli, F. Andreani, F. Decker, *Electrochim. Acta* **44**, 4189 (1999)
25. M. Weis, K. Lee, D. Taguchi, T. Manaka, M. Iwamoto, *Synth. Methods* **162**, 2236 (2012)
26. E.C.R. Maia, D.C. Bento, E. Laureto, D.A.M. Zaia, E.M. Therézio, G.J. Moore, H. De Santana, *J. Serbian. Chem. Soc.* **78**, 507 (2013)
27. D.C. Bento, E.C.R. Maia, T.N.M. Cervantes, C.A. Olivati, G. Louarn, H. De Santana, *J. Mater. Sci. Mater. Electron.* **26**, 149 (2015)
28. E.M. Therézio, J.L. Duarte, E. Laureto, E. Di Mauro, I.L. Dias, A. Marletta, H. de Santana, *J. Phys. Org. Chem.* **24**, 640 (2011)
29. H. Koizumi, H. Dougauchi, T. Ichikawa, *J. Phys. Chem. B* **109**, 15288 (2005)
30. D.C. Bento, E.C.R. Maia, R.V. Fernandes, E. Laureto, G. Louarn, H. de Santana, *J. Mater. Sci. Mater. Electron.* **25**, 185 (2014)
31. M. Lapkowski, K. Berrada, S. Quillard, J.G. Louarn, S. Lefrant, A. Pron, *Macromolecules* **28**, 1233 (1995)
32. J. Laska, A. Pron, S. Lefrant, *J. Polym. Sci. Polym. Chem.* **33**, 1437 (1995)
33. H. de Santana, S. Quillard, E. Fayad, G. Louarn, *Synth. Methods* **156**, 81 (2006)
34. D.C. Bento, E.C.R. Maia, P.R.P. Rodrigues, G. Louarn, H. de Santana, *J. Mater. Sci. Mater. Electron.* **24**, 4732 (2013)
35. G. Lillie, P. Payne, P. Vadgama, *Sens. Actuators B* **78**, 249 (2001)
36. E.M. Giroto, M.A. De Paoli, *Quim. Nova* **22**, 358 (1999)
37. H. de Santana, F.C. Dias, *Mater. Chem. Phys.* **82**, 882 (2003)
38. M. Ates, T. Karazehir, F. Arican, N. Eren, *J. Coat. Technol. Res.* **10**, 317 (2013)
39. Y.D. Park, D.H. Kim, Y. Jang, J.H. Cho, M. Hwang, H.S. Lee, J.A. Lim, K. Cho, *Electronics* **7**, 514 (2006)
40. K. Yoshino, S. Morita, M. Uchida, K. Muro, T. Kawai, Y. Ohmori, *Synth. Methods* **55**, 28 (1993)
41. H.S. Lee, J.H. Cho, K. Cho, Y.D. Park, *J. Phys. Chem. C* **117**, 11764 (2013)
42. D. Momodu, A. Bello, J. Dangbegnon, F. Barzeger, M. Fabiane, N. Manyala, *J. Solid State Electrochem.* **19**, 445 (2015)
43. G. Louarn, J.-Y. Mevellec, J.P. Buisson, S. Lefrant, *Synth. Methods* **55**, 587 (1993)
44. M.S.A. Abdou, F.P. Orfino, Y. Son, S. Holdercroft, *J. Am. Chem. Soc.* **119**, 4518 (1997)